VOLUME 3, NUMBER 3 JULY / SEPTEMBER 2000

IFSCC magazine

The Global Publication of the International Federation of Societies of Cosmetic Chemists

Reprint

Roger L. McMullen, Janusz Jachowicz, and Stephen P. Kelty

Correlation of AFM/LFM with Combing Forces of Human Hair

INTERNATIONAL FEDERATION IFSCC SOCIETIES OF COSMETIC CHEMISTS

Correlation of AFM/LFM with Combing Forces of Human Hair

Roger L. McMullen*+, Janusz Jachowicz*, and Stephen P. Kelty+

Abstract

A comparative study is presented of dry combing forces measured with a Miniature Tensile Tester and micron-scale frictional forces measured using Normal and Lateral Force Microscopy of virgin and treated human hair. Topographic images of the fibers show the presence of small pores, which become increasingly prevalent upon solvent extraction. The pores appear to attract cationic polymers. Friction images show surface variations that are interpreted as areas of varying lipid film coverage. Friction image analysis indicates a good correlation of image data and combing forces as measured with a modified Miniature Tensile Tester.

Introduction

Recent investigations of hair fiber surface features using Atomic Force Microscopy (AFM) and other complementary Scanning Probe Microscopy (SPM) techniques have shown that this class of surface sensitive techniques is particularly well suited for probing the local surface properties of natural fibers from the atomic to micron scale. For example, a considerable amount of interest has focused on quantifying the cuticle step heights of human hair [1-3], and characterizing the surface roughness of the morphological components of the cuticle, i.e. the exocuticle, endocuticle, and the A-layer [3]. Additionally, these studies have demonstrated the use of AFM to study hair at various degrees of hydration [1-3] and at a range of pH levels [3, 4]. Other studies, primarily interested in the adsorption of cationic polymers onto hair, have also been completed [5-8]. More recently, *Parbhu* et al. [9] used force-volume and nano-indentation techniques to measure the hardness and relative elastic moduli of the morphological components of the wool fiber. Their results were in agreement with what one would expect considering the chemical composition of the various components of the wool fiber.

In AFM, one obtains a topographical image by measuring the vertical deflection of a soft cantilever, to which the tip is attached, as the tip is rastered over the surface [10]. The cantilever deflections normal to the surface are representative of topographical surface features. In addition to AFM, Lateral Force Microscopy (LFM) is a complementary technique in which the torsional twisting the tip and cantilever is measured to provide a measure of the drag or friction of the tip on the surface [11-13]. LFM can be used to study the frictional drag properties of hair fibers at the local level and thus provide a fundamental understanding of the underlying properties which lead to macroscopic combing forces. Although several AFM investigations on human hair fibers have recently appeared in the literature, to our knowledge, complementary LFM studies have not been forthcoming. However, there has been a limited amount of information reported concerning the LFM of wool fibers in which different frictional domains were observed in oxidized samples [14, 15].

We herein report combined AFM and LFM investigations of various types of hair fibers including virgin, chemically treated (bleached), delipidized (by solvent extraction), and polymer treated hair. All modified hair types show an increase in dry combing forces as quantified by combing measurements carried out for fiber assemblies by employing a Miniature Tensile Tester equipped with a special accessory for combing measurements. We attempt to correlate combing data with the observed changes in hair surface morphology and friction.

Experimental Details

AFM/LFM Instrumentation

AFM and LFM studies were performed using an AutoProbe™ CP manufactured by Park Scientific Instruments. An AFM/LFM probe head was used in conjunction with a 100 µm piezoelectric scanner, operating in the contact mode. The instrument used was the »beam-bounce« type in which a diode laser beam is focused onto the back (top) of the cantilever. The variation in the angle of reflection is used to monitor the normal and torsional cantilever deflection by means of a four-quadrant position sensitive photodetector. Commercial gold-coated Si_3N_4 cantilevers with pyramidal tips (microlevers) were used in the analysis. **Fig. 1** shows a general scheme of a scanning probe microscope. As seen in this figure, an optical lever detection system is used to monitor the cantilever deflection as a result of interactions between the tip and the analyzed sample. We operated the instrument in constant force mode, in which the sample vertical height is continuously adjusted via an electronic feedback loop so that the probe maintains a constant force with the sample. Therefore, changes in topography that result in cantilever deflection will cause the feedback loop to signal the piezoelectric scanner and change the position of the sample.

Materials and Procedures

In this study we compare virgin with solvent-extracted and bleached hair. Oriental human hair (International Hair Importers & Products, Inc.) was used for all investigations due to its high radius of curvature as compared to other hair types, which facilitates sur-

+ Department of Chemistry and Biochemistry, Seton Hall University, South Orange, NJ, USA
* International Specialty Products, Wayne, NJ, USA

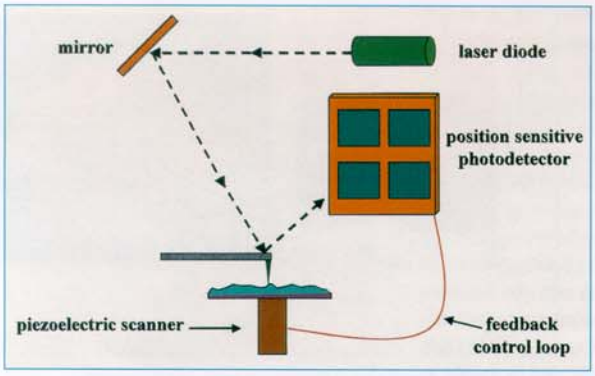

Fig. 1 General scheme of a scanning probe microscope; adapted from *Howland* et. al. [16]

face scanning in the AFM/LFM instrument. Virgin hair, as supplied by the distributor, was compared with hair extracted with a series of solvents. The effect of solvent extraction on hair was investigated first by treatment with *t*-butanol and n-hexane, each for 4 hours, then with a mixture of chloroform/methanol (70:30 v/v) for 6 hours. In each procedure, 3 g of hair was treated with 250 mL of solvent in a Soxhlet extractor. Additionally, we examined the effect of bleaching hair by using a commercial product consisting of Clairol Professional BW 2 bleaching powder and Emiliani Professional 20 Volume clear developer.

The cationic polymer, co(vinyl pyrrolidone-methacrylamidopropyl trimethylammonium chloride) [PVP/MAPTAC], was employed to modify the surface properties of hair. It is a commercial product sold under the trade name of Gafquat HS-100. Treatment of hair with this material consisted of soaking hair in a 1% polymeric solution followed by rinsing and drying.

For AFM studies, virgin and treated hair fibers were mounted to steel sample studs using nail polish. Attempts to use epoxy or other adhesives, which have been used in other studies, indicated a tendency to wet the fibers, particularly at the cuticle edge. Consequently, images of fibers obtained using epoxy may be considered suspect. In contrast, typical nail polish showed no tendency to wet the fiber surface but did offer good stability. All image data presented in this report are raw and unfiltered, unless otherwise noted. In normal operation, the difference between actual cantilever deflection and a reference setpoint is supplied to a feedback loop connected to the z-drive (height) of the scanner. The voltage supplied to the z-drive is the origin of the topographic image data and is sensitive to topographic surface features. The error signal image reflects the difference between the actual cantilever deflection and the setpoint, and is highly sensitive to changes in height. Consequently, we found that it is useful to monitor both the topographic and error signal simultaneously since they are complementary data sets. LFM data were obtained in both scan directions providing us with two complementary images, illustrating the torsional bending experienced by the cantilever in the forward and reverse scan directions.

Combing measurements of hair tresses were performed using a Miniature Tensile Tester (Dia-Stron Ltd.) operated by MTTWIN 4.1a software. The combing analysis of untreated and chemically modified hair is presented. Experimental procedures are similar to those described previously [17].

Lateral force measurements in combination with AFM can provide fundamental information about the physical and chemical properties of the surface. Soft materials, such as gels and waxes, allow the tip to penetrate the surface resulting in an increase in drag coefficient, which, in turn, causes the cantilever to experience greater torsion. In contrast, hard crystalline materials do not allow the tip to penetrate the surface as much, so a lower drag coefficient results typically characterized by lower friction. Besides surface chemical composition, friction may also result from topographical features such as pores or pits especially if these features have radii comparable or smaller than the tip radius. In order to distinguish the lateral forces contributed by surface chemical properties and topographical features, we record simultaneous images of the topography and lateral deflection. Furthermore, the frictional force F_f experienced by the tip is dependant on both the frictional coefficient μ and the loading force F_l [18].

$$F_f = \mu \cdot F_l \quad (1)$$

To calculate the friction from LFM measurements, other factors including the shape and composition of the tip as well as the design and physical characteristics of the cantilever must be known. In general, these details are not sufficiently known in a given experiment to accurately calculate the friction. However, the relative variation in friction may be used to provide meaningful comparisons among various sample surfaces. To accomplish this, the effects of loading force must be eliminated from the comparison. A convenient method to accomplish this is to measure the friction signal as a function of loading force. Another effect which must be accounted for when comparing different samples is that the measured value of the friction signal is highly dependent on instrument parameters which vary from one scan setup to the next. These variations can also be eliminated by taking the difference between forward and reverse scans. During each scan, images were obtained for the topographic, error signal, LFM-forward, and LFM-reverse measurements simultaneously.

Results & Discussion

A typical set of topographic, error signal, LFM-forward, and LFM-reverse images is shown in **Fig. 2**. These images were obtained

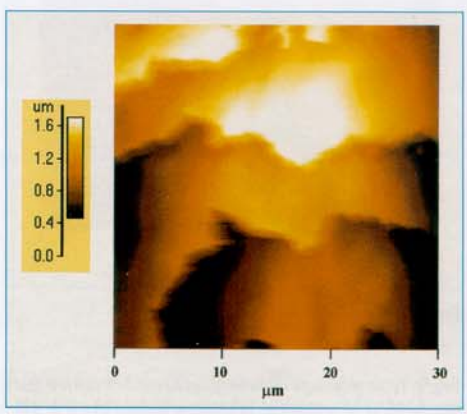

Fig. 2a

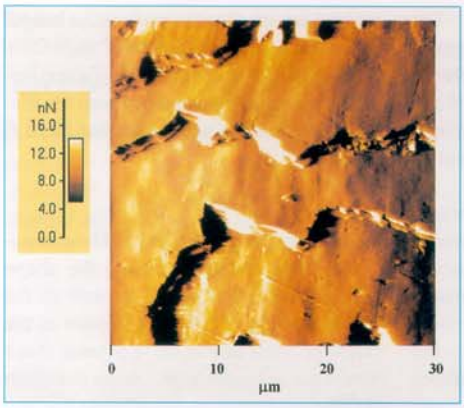

Fig. 2b

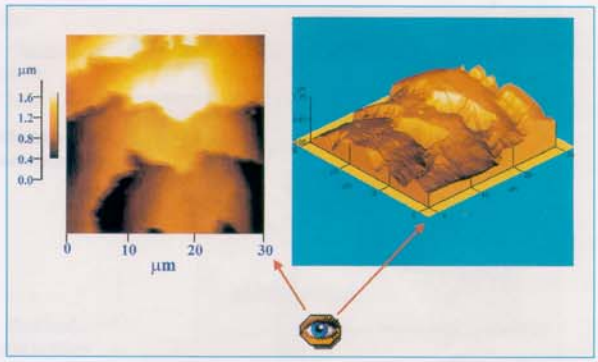

Fig. 3 Three-dimensional representation of topography

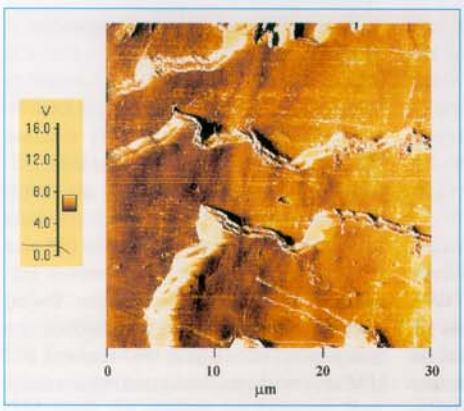

Fig. 2c

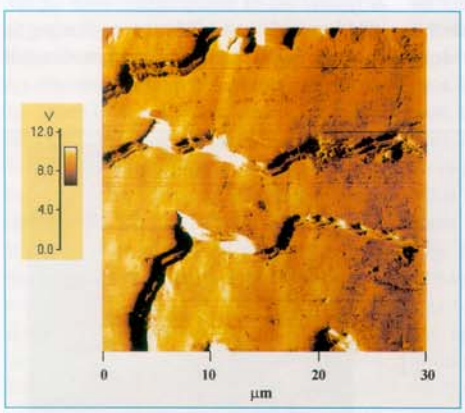

Fig. 2d

Fig. 2 Typical image data scans (30 mm) obtained during AFM/LFM analysis: (a) topography, (b) error signal, (c) LFM-Forward, (d) LFM-reverse

simultaneously for a 30 µm scan (900 µm^2 scan area) on untreated hair. The scale in **Fig. 2a** correlates darker colored areas with lower topography and lighter colored areas with regions of higher topography. **Fig. 3** shows the topographic data of **Fig. 2a** in a three-dimensional format. The LFM data, depicted in **Figs. 2c** and **2d**, illustrates the torsional bending of the cantilever as it rasters across the sample in each directions. It is important to note that what appears dark in **Fig. 2c**, transpires as light in **Fig. 2d** and vice-versa. In **Fig. 2c** (LFM-forward), dark represents areas that are higher in friction whereas light is indicative of lower frictional regions. The opposite is true for **Fig. 2d** (LFM-reverse), in which light corresponds to high friction and dark represents low friction. By taking the difference between **Figs. 2c** and **2d**, one can obtain relative frictional information about a particular material. However, the images must be collected at various normal forces in order to obtain a plot of torsional cantilever deflection as a function of the set point. The slope of this plot provides a value related to the coefficient of friction between the probe tip and the sample.

When comparing the virgin, bleached, and solvent extracted hair we found that virgin hair, as supplied from the manufacturer, was often characterized by the presence of small micro-deposits on the surface. After solvent extraction or bleaching the deposits were found to be less predominant. **Fig. 4** provides an (a) error signal (b) LFM-forward, and an (c) LFM-reverse scan image, most representative of those found for virgin hair. The images provide evidence for the presence of particles, in which case some of the particles may be classified as being frictionally different than the rest of the hair surface since the entire particle has a different color in the LFM images than the remaining hair surface. Also prevalent are donut shaped features, which occur as opposing colors in the LFM forward and reverse images. As stated previously, lighter

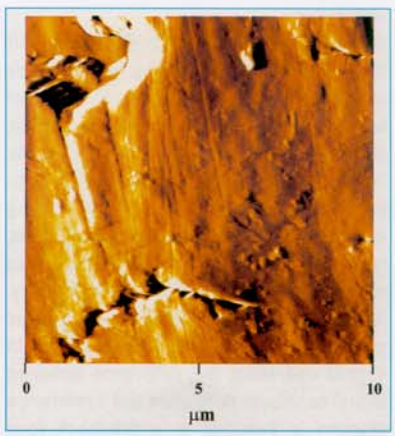

Fig. 4a

Fig. 4b

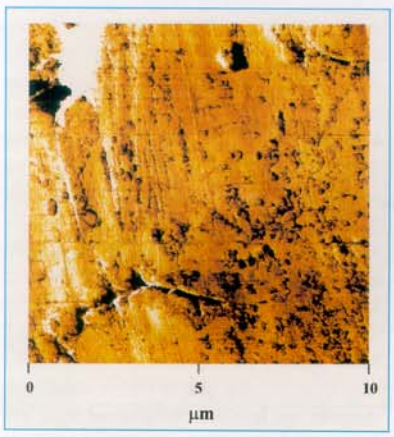

Fig. 4c

Fig. 4 (a) Error signal, (b) LFM-forward, and (c) LFM-reverse images (10 mm) for virgin hair, illustrating surface deposits on hair

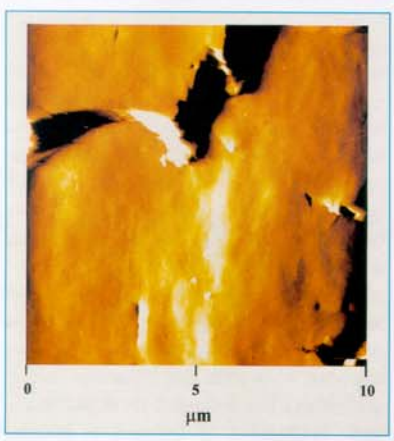

Fig. 5a

colors in the LFM-forward image correspond to larger degrees of cantilever torsion while darker colors in the LFM-reverse image correspond to larger degrees of torsion. This would mean that the particles might be made of a softer material than the remaining surface. If this is the case, it is possible that the particles represent soft surface deposits on the hair, such as sebum. Hair that has undergone Soxhlet extraction with the selected solvents does not possess the higher friction particles as shown by the AFM and LFM images in **Fig. 5**. Similarly, analysis of bleached hair also suggests that most of such particles are removed during this chemical treatment.

Another striking feature of the hair surface was the presence of a large quantity of micro-pores. **Fig. 6** provides a representative site on solvent extracted hair in which a considerable population of micro-pores can be seen. The average diameter of the pores was determined to be 149 nm ± 24 nm with their depth estimated to be 7.94 nm ± 2.45 nm. As stated in **Table 1**, the micro-pores were found in 21% of the sites examined in virgin hair, 42% in bleached, and 70% in solvent extracted hair. These features may be interpreted as surface damage; however, there presence in both virgin and treated fibers indicates that they may occur naturally on the fiber surface. As a result of oxidative/alkaline treatment or solvent extraction, many of the surface lipids are dissolved/solubilized and removed, revealing the actual hair surface with micro-pores present. We attribute their increased occurrence in bleached and solvent extracted hair as resulting from dissolution of the surface lipids and exposure of the fiber surface. To our knowledge, reports of the micro-pores have not appeared in the literature, however, their presence is occasionally evident in unpublished hair micrographs [19]. It is also probable that micro-pores have not been previously observed in most scanning electron microscope (SEM) studies, since a 10 nm coating of gold is usually sputtered on the hair sample in order to make it electro-conductive, a layer that could effectively mask the presence of surface features such as micro-pores [14]. The images of virgin hair, shown in **Fig. 4**, demonstrate the

Fig. 5b

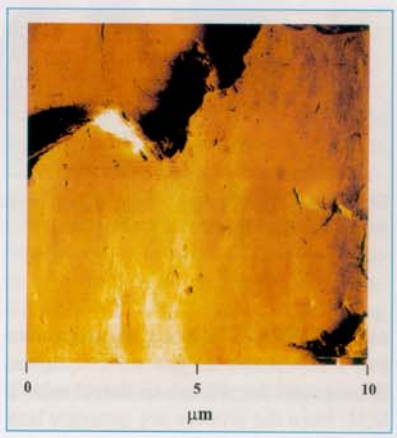

Fig. 5c

Fig. 5 (a) Error signal, (b) LFM-forward, and (c) LFM-reverse images (10 mm) for solvent extracted hair

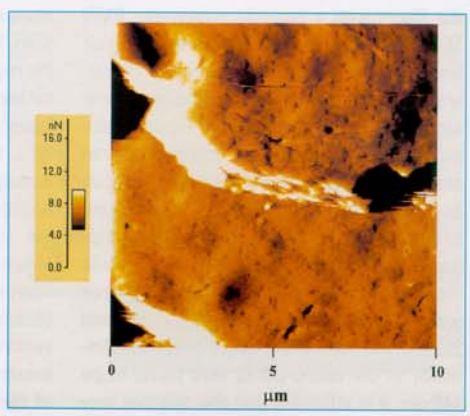

Fig. 6 Error signal image (10 µm) of solvent extracted hair revealing micro-pores on the hair surface

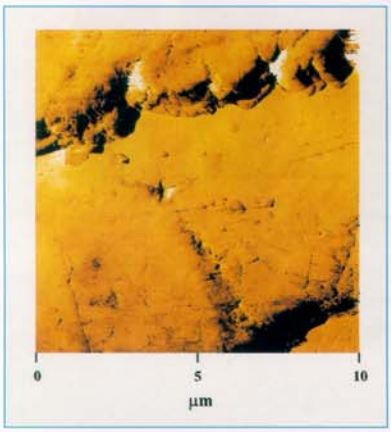

Fig. 9b

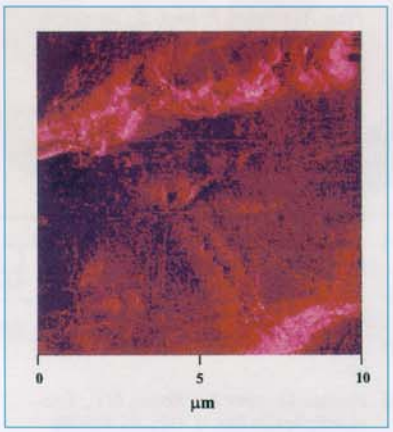

Fig. 9c

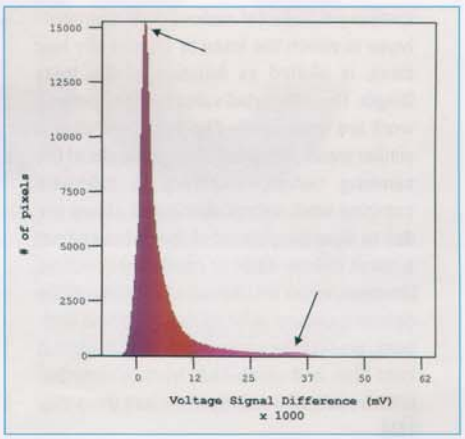

Fig. 9d

Fig. 9 (a) LFM forward, (b) LFM reverse, (c) Difference Image, and (d) Difference Image histogram for a 10 µm scan of solvent extracted hair

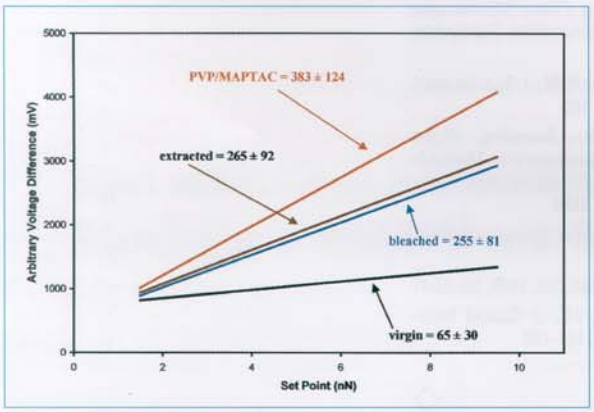

Fig. 10 Arbitrary voltage difference as a function of set point (normal force) for various hair treatment protocols. The average slope is reported for each data set

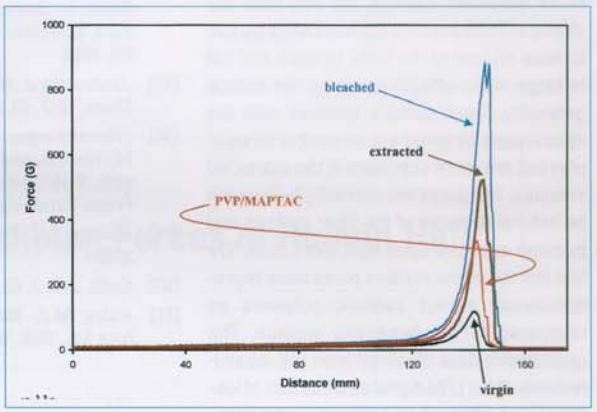

Fig. 11a

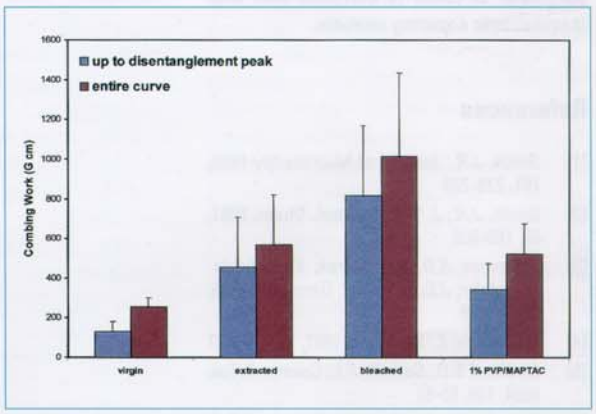

Fig. 11b

Fig. 11 Force as a function of tress distance corresponding to (a) dry combing curves for hair that has undergone the indicated treatment protocols as well as (b) the integrated values obtained for the curves

surface, with the exception of the cuticle edge. This is a more informative parameter than an average, which takes into account all signal difference values.

To understand the frictional differences between virgin, solvent extracted, bleached, and polymer treated hair, images were collected from various surface regions and at a series of loading forces. A plot of signal difference as a function of loading force F_l allows us to determine the slope of that relationship, thereby yielding a parameter directly related to the coefficient of friction for a Si_3N_4 tip sliding on a particular hair surface **(Fig. 10)**. The slopes for each hair type as well as the standard deviation for each series of measurements are indicated in the figure. The smallest slope is obtained by virgin followed by bleached, solvent extracted, and polymer treated hair. These results are consistent with dry combing values obtained experimentally with a Dia-Stron Miniature Tensile Tester. **Fig. 11a** presents the dry

combing curves for various hair treatment types in which the force to comb a dry hair tress, is plotted as function of the tress length. The integrated values of the combing work are compiled in **Fig. 11b**, illustrating a similar trend. Arguably, the end peaks of the combing curves, employed to calculate combing work values discussed above are due to disentanglement of the fibers and not a result of inter-fiber or comb-fiber friction. However, when we integrate the region of the combing curves prior to the observed end-peak, we find the same trend, indicating that inter-fiber and comb-fiber friction contribute to the overall combing of the hair tress **(Fig. 11b)**.

Concluding Remarks

In all materials studied, we find that the effects of increased friction are invariably due to local effects of the fiber surface and not to large-scale effects involving the cuticle geometry. Small surface features with the appearance of pores are evident in all samples but are more prevalent in the extracted samples. The pores are currently believed to be natural features of the fiber surface and become exposed upon lipid extraction. We find that the edges of these pores seem to predominantly attract cationic polymers as compared to the remaining surface. The quantitative data obtained from the measurements of the LFM signal as a function of loading force allowed an estimation of a parameter related to fiber-probe friction. This parameter is found to correlate well with macroscopic combing analysis.

References

[1] *Smith, J.R.;* Journal of Microscopy 1998, 191, 223-228

[2] *Smith, J.R.;* J. Soc. Cosmet. Chem. 1997, 48, 199-208

[3] *O'Connor, S.D.; Komisarek, K.L.; Baldeschwieler, J.D.;* J. Invest. Dermatol. 1995, 105, 96-99

[4] *You, H.; Yu, L.;* Scanning 1997, 19, 431-437

[5] *Goddard, E.D.; Schmitt, R.L.;* Cosmet. & Toil. 1994, 109, 55-61

[6] *Schmitt, R.L.; Goddard, E.D.;* Cosmet. & Toil. 1994, 109, 83-93

[7] *Hössel, P.; Sander, R.; Schrepp, W.;* Cosmet. & Toil. 1996, 111, 57-65

[8] *Pfau, A.; Hössel, P.; Vogt, S.; Sander, R.; Schrepp, W.;* Macromol. Symp. 1997, 126, 241-252

[9] *Parbhu, A.N.; Bryson, W.G.; Lal, R.;* Biochemistry 1999, 38, 11755-11761

[10] *Magonov, S.; Whangbo, M.-H.:* Surface Analysis with Scanning Tunneling and Atomic Force Microscopy; VCH: Weinheim, Germany, 1996

[11] *Neumeister, J.M.; Ducker, W.A.;* Rev Sci Instr 1994, 65, 2527-2531

[12] *Hamers, R.J.;* Journal of Physical Chemistry 1996, 100, 13103-13120

[13] *Den, B.A.;* J Rev. Sci. Instrum. 1990, 62, 88-92

[14] *Phillips, T.L.; Horr, T.J.; Huson, M.G.; Turner, P.S.;* Textile Res. J. 1995, 65, 445-453

[15] *Crossley, J.A.; Gibson, C.T.; Mapledoram, L.D.; Huson, M.G.; Myhra, S.; Pham, D.K.; Sofield, C.J.; Turner, P.S.; Watson, G.S.;* Micron 2000, 31, 659-67

[16] *Howland, R.; Benatar, L.;* A Practical Guide to Scanning Probe Microscopy; Park Scientific Instruments: Sunnyvale, CA, 1996

[17] *Jachowicz, J.; Helioff, M.;* J. Soc. Cosmet. Chem. 1997, 48, 93-105

[18] *Wiesendanger, R.:* Scanning Probe Microscopy and Spectroscopy: Methods and Applications; Canmbridge Unv. Press: Cambridge, 1994

[19] *Garcia, M.;* Personal Communication, 2000

[20] *Swift, J.A.;* J. Cosmet. Sci. 1999, 50, 23-47

[21] *Hafey, M.J.; Watt, I.C.;* J. Colloid Interface Sci. 1986, 109, 181-189

◇